RESEARCH ARTICLE

Magnetic Resonance Imaging Visualization of Vulnerable Atherosclerotic Plaques at the Brachiocephalic Artery of Apolipoprotein E Knockout Mice by the Blood-Pool Contrast Agent B22956/1

Cinzia Parolini, Marco Busnelli, Giulia S. Ganzetti, Federica Dellera, Stefano Manzini, Eugenio Scanziani, Jason L. Johnson, Cesare R. Sirtori, and Giulia Chiesa

Abstract

The aim of this study was to identify, by magnetic resonance imaging (MRI), the ability of the blood-pool contrast agent B22956/1 to detect atherosclerotic plaques developing at the brachiocephalic artery of apolipoprotein E knockout (apoE-KO) mice and to possibly identify vulnerable atherosclerotic lesions. After high-fat feeding for 8 or 12 weeks, MRIs of brachiocephalic arteries were acquired before and after B22956/1 administration; then vessels were removed and analyzed by histology. B22956/1 injection caused a rapid increase in plaque signal enhancement and plaque to muscle contrast values, which remained stable up to 70 minutes. A linear correlation between signal enhancement and macrophage content was found 10 minutes after B22956/1 injection ($p < .01$). Signal enhancement and plaque to muscle contrast values correlated with macrophage content 40 minutes after contrast agent administration ($p < .01$). Finally, 70 minutes after B22956/1 infusion, plaque to muscle contrast significantly correlated with the percentage of stenosis ($p < .005$). B22956/1 administration to high fat–fed apoE-KO mice resulted in a rapid enhancement of atherosclerotic plaques and in a great ability to rapidly visualize vulnerable plaques, characterized by a high macrophage content. These results suggest that B22956/1 could represent an interesting tool for the identification of atherosclerotic plaques potentially leading to acute cardiovascular events.

ATHEROSCLEROSIS is the underlying pathology of the majority of cardiovascular diseases and is still the leading cause of morbidity and mortality in Western countries.[1] Atherosclerosis is usually complicated by acute thrombosis and is frequently triggered by the rupture of an atherosclerotic plaque, which in turn leads to acute ischemic events.[2] Rupture-prone plaques, defined as vulnerable plaques, are characterized by having few smooth muscle cells (SMCs), many inflammatory cells, particularly macrophage-derived foam cells, a large lipid pool, and a thin fibrous cap.[2–4] Disruption of the thin fibrous cap of such vulnerable plaques causes the direct contact of blood coagulation factors to tissue factor and can trigger occlusive thrombus formation.[5]

The apolipoprotein E knockout (apoE-KO) mouse is widely recognized as a model of hypercholesterolemia that spontaneously develops atherosclerotic lesions, even on a standard chow diet with low fat content and no cholesterol.[6] Atherogenesis in this model is strongly accelerated by a high-fat, high-cholesterol diet.[7] ApoE-KO mice are unique animal models of atherosclerosis for their resemblance to the human counterpart because they develop vascular lesions over time, starting from initial fatty streaks up to complex lesions, characterized by a necrotic lipid core and a fibrous cap.[7,8] In addition, when fed a Western diet, apoE-KO mice develop acute atherosclerotic plaque disruption in the brachiocephalic artery, a very short, narrow vessel that originates from the aortic arch, branching to form the right subclavian artery and the right common carotid artery.[9–11]

From the Departments of Pharmacological and Biomolecular Sciences and Veterinary Science and Public Health, Università degli Studi di Milano, Milan, Italy, and Bristol Heart Institute, University of Bristol, Bristol, UK.

Address reprint requests to: Giulia Chiesa, PhD, Department of Pharmacological and Biomolecular Sciences, Università degli Studi di Milano, via Balzaretti 9, 20133 Milano, Italy; e-mail: Giulia.Chiesa@unimi.it; Cinzia Parolini, PhD, Department of Pharmacological and Biomolecular Sciences, Università degli Studi di Milano, via Balzaretti 9, 20133 Milano, Italy; e-mail: Cinzia.Parolini@unimi.it.

DOI 10.2310/7290.2014.00012

Magnetic resonance imaging (MRI) has emerged as the most promising technique for studying atherosclerosis in vivo in humans and in animal models because it is accurate, reproducible, noninvasive, and safe and does not require ionizing radiation.[12] The introduction of paramagnetic contrast agents has further improved plaque characterization and has been used to characterize plaques in terms of fibrocellular tissue, lipid core, and intraplaque hemorrhage; to enhance visualization of the fibrous cap; and to evaluate biologic processes such as inflammation and neovascularization in different types of atherosclerotic lesion.[13–17] The gadocoletic acid trisodium salt (B22956/1) is a gadolinium (Gd)-based MRI contrast agent. It is a so-called blood-pool contrast agent due to the prolonged presence in the vasculature, originating from its high affinity for serum albumin.[18] This contrast agent has already been proven to enhance the visualization of atherosclerotic plaques in balloon-injured rabbits.[19] However, its use has not been applied to the identification of human-like atherosclerotic plaques, that is, apoE-KO mouse plaques, and particularly to the visualization of rupture-prone arterial lesions, such as plaques developing at the brachiocephalic artery.

The aim of this study was to evaluate, by MRI, the ability of the contrast agent B22956/1 (1) to detect atherosclerotic plaques developing at the brachiocephalic artery of apoE-KO mice and (2) to identify, in vivo, those plaques with histologic features associated with high vulnerability. To this aim, possible correlations between MRI data and histologic quantification of plaque components were evaluated.

Materials and Methods

Animals

Sixteen male apoE-KO mice in a C57BL/6J genetic background and six male C57BL/6J mice as controls, 7 weeks old, were purchased from Charles River Laboratories (Calco, Italy).

At 8 weeks of age, mice were switched from a standard rodent diet to a high-fat diet containing 21% (wt/wt) fat from lard and supplemented with 0.15% (wt/wt) cholesterol (Special Diets Services, Essex, UK). Mice were equally distributed into two groups: the first group was fed the high-fat diet for 8 weeks, whereas the second group received the diet for 12 weeks.

Procedures involving animals and their care were conducted in accordance with institutional guidelines that are in compliance with national (D.L. No. 116, G.U. Suppl. 40, February 18, 1992, Circolare No. 8, G.U. July 1994) and international laws and policies (EEC Council Directive 2010/63, September 22, 2010: Guide for the Care and Use of Laboratory Animals, United States National Research Council, 2011).

Contrast Agent

Gadocoletate trisodium (Lab. Code B22956/1, Bracco Imaging SpA, Milan, Italy) is a derivative of gadopentetate bearing on the methylene group of the centrally located acetate group in *S*-configuration, a propionic acid linker to the amino group of the 3β-amino analogue of deoxycholic acid. Its chemical name according to CAS # 280776-87-6 is trisodium [(3*β*,5*β*,12*α*)-3-[[(4*S*)-4-[bis[2-[bis[(carboxy-k*O*)methyl]amino- k*N*]ethyl]aminok*N*]-4-(carboxy-k*O*))-1-oxobutyl]amino]-12-hydroxycholan-24-oato(6-)]gadolinate(3-), and the proposed nonproprietary name (INN) is gadocoletic acid trisodium salt.[18] It has the composition $C_{41}H_{60}N_4O_{14}GdNa_3$, with a molecular weight of 1059.17 Da. It is a hygroscopic off-white solid, and its structure is shown in Figure 1. Its apparent relaxivity is 27 $mM^{-1}s^{-1}$, as determined by measuring the relaxation rate of a 0.6 mM solution of the chelate in Seronorm at 0.5 T.[19]

MRI Experiments

MRI experiments were performed on apoE-KO and C57BL/6J mice using a Bruker PharmaScan scanner (Bruker Italia, Milan, Italy) dedicated to small rodents, equipped with a 7 T/16 cm magnet and a ^1H 38 mm birdcage radiofrequency coil. For the duration of the scans, animals were kept under controlled anesthesia conditions (about 33% O_2, 66% N_2O, and 1% isoflurane).

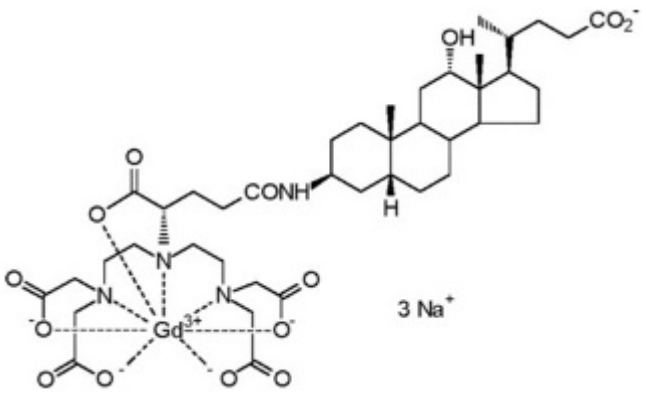

Figure 1. Molecular structure of gadocholetic acid trisodium salt (B22956/1).

The accurate localization of the brachiocephalic artery was obtained using gradient echo fast imaging sequences, which allowed precise definition of the pseudocoronal plane where the vessel of interest lies, as well as its orientation within the plane. Acquisition parameters were set as follows: repetition time (TR) = 75 ms, echo time (TE) = 3 ms, number of averages (NA) = 4, flip angle = 40°, field of view (FOV) = 3.5 × 3.0 cm^2, matrix size (MS) = 128 × 128, and slice thickness = 1.5 mm.

To detect and properly quantify the enhancement induced by the contrast agent in the plaques (or in the vessel walls for healthy mice), a slab covering the brachiocephalic artery was imaged for each animal, using a three-dimensional T_1-weigthed fast spin echo sequence with the following parameters: TR = 400 ms, TE = 13 ms, NA = 1, FOV = 3.0 × 3.0 × 0.4 cm^3, MS = 256 × 256 × 8, and segmentation factor = 2. Spin echo–based sequences intrinsically attenuate the signal of flowing spins ("black blood" effect), thus allowing a more reliable measurement of the enhancement occurring in the proximity of the lumen. It is worth noting, however, that such attenuation can be rather moderate when spins are moving slowly, as happens at the vessel boundaries. Thus, to avoid artifacts due to unsaturated spins flowing through the observed slab, the black blood effect was maximized by triggering on the systolic phase of the electrocardiogram. T_1-weighted images were acquired for each animal before bolus injection of B22956/1 (dose 0.1 mmol/kg, rate 4 mL/min) and 10, 20, 30, 40, 50, 60, and 70 minutes after the administration of the contrast agent.

MRI Analysis

A 0.5 mm slice of the brachiocephalic artery, starting from its aortic arch branching point, was selected and analyzed before and at different time intervals after contrast agent injection. Images affected by motion artifacts were discarded. Two regions of interest (ROI) were manually selected:

- Plaque: the region of the brachiocephalic artery, recognized as an atherosclerotic plaque or a region with comparable area, selected as a healthy reference area
- Muscle: a homogeneous region of the animal foreleg

ROI were selected by operators blinded with respect to animal identity and histology output using a custom-made tool developed within *ImageJ* software (National Institutes of Health, Bethesda, MD). ROI plaque was drawn in a region of the brachiocephalic artery on the base of vessel shape and postcontrast enhancement. To include animals with no recognized pathology into the analysis, a region with shape and area comparable to the plaque ROI was placed over the artery wall.

The signal evolution of the plaque was evaluated, at each time point, as signal enhancement (SE) and plaque to muscle contrast (PMC) of ROI, defined as follows:

$$\text{Signal Enhancement } \%(t) = \frac{S_{plaque}(t) - S_{plaque}(0)}{S_{plaque}(0)} \times 100$$

$$\text{Plaque to Muscle Contrast } \%(t) = \frac{S_{plaque}(t) - S_{muscle}(t)}{S_{muscle}(t)} \times 100$$

where t is the time point and S(t) and S(0) are the mean signal intensity at time t and precontrast, respectively.

Image analyses were performed with *ImageJ* 1.46 software by two independent observers, blinded to the histology results.

Histology and Immunohistochemistry

After the MRI acquisitions, animals were anesthetized by intramuscular injection of tiletamine/zolazepam (Zoletil) 0.4 mL/kg and xylazine (Rompun) 0.25 mL/kg and then exsanguinated by arterial perfusion via the abdominal aorta with phosphate-buffered saline with outflow through the incised jugular veins, followed by perfusion with 4% formalin. Brachiocephalic arteries were then removed and embedded in paraffin. Serial 5 μm sections were cut starting from the aortic branching point; to make a comparison between histologic features and MRI data, the sections in the first 0.5 mm of the brachiocephalic arteries were stained with hematoxylin (Mayer's Haemalum, Bio-Optica, Milano, Italy) and eosin (Bio-Optica, Milano, Italy), with the neighboring sections stained with Masson's trichrome (Bio-Optica, Milano, Italy) or used for the detection of macrophages and SMCs. Macrophages and SMCs were detected using an anti-F4/80 antibody (ab6640, Abcam, Cambridge, UK) and an antibody specific for the α-smooth muscle actin (A5228, Sigma-Aldrich, St. Louis, MO), respectively. A biotinylated secondary antibody was used for streptavidin-biotin-complex peroxidase staining (Vectastain Abc Kit, Vector Laboratories, Peterborough, UK). 3,3′-Diaminobenzidine was used as chromogen (Sigma-Aldrich), and sections were counterstained with hematoxylin (Mayer's Haemalum). The plaque lipid content of delipidated paraffin sections was measured as previously described.[20] Briefly, sections were digitally processed into monochrome so that the plaque area occupied by

lipids appeared as an empty white area surrounded by black tissue. Thus, the fractional lipid content was measured as the percentage of the total white area over the total plaque area.

Morphometric and Immunohistochemical Analyses

The Aperio ScanScope GL Slide Scanner (Aperio Technologies, Vista, CA), equipped with a Nikon 20x/0.75 Plan Apochromat objective producing a 0.25 μm/pixel scanning resolution and the Aperio *ImageScope* software (version 8.2.5.1263), was used to acquire and process digital images with a 40× magnification.

Each hematoxylin and eosin–stained section was analyzed to measure plaque area, percentage of stenosis, lipid content, and fibrous cap thickness. Masson's trichrome–stained sections were analyzed for extracellular matrix (ECM) content, whereas immunohistochemical stained sections were evaluated for the SMC and macrophage content. These parameters were measured as plaque area occupied by ECM, SMC, or macrophages/total plaque area × 100. An operator blinded to the MRI results performed these histologic quantifications.

Statistical Analysis

The following methods were applied to analyze MRI and histologic data. If continuous variable distributions had to be compared across categorical variables levels, the Student *t*-test was applied. Changes in MRI parameters over time were tested for statistical significance by multivariate analysis of variance (repeated measures), followed by the Tukey post hoc test; a value of $p < .05$ was considered statistically significant. When the relation between two or more categorical variables had to be analyzed, cross-tabulation (also referred to as a contingency table) was used. The significance of correlation was calculated with the Pearson chi-square test. To assess that two continuous variables were linearly correlated, the significance of the Pearson correlation was computed. For the statistical analyses, *SPSS* software, PASW Statistics 18, release version 18.0.0 (IBM Corporation, Armonk, NY), and *Systat* 13 software (Systat Software, San Jose, CA) were used.

Results

Histologic and Immunohistochemical Analyses

As expected, control C57BL/6J mice did not develop atherosclerotic lesions at both 8 and 12 weeks of high-fat feeding (data not shown). On the contrary, 14 of 16 apoE-KO mice developed fibrofatty atherosclerotic lesions at the brachiocephalic artery at both time points. SMCs were localized in the fibrous cap, whereas macrophages were mostly found surrounding the necrotic core of atheromas, colocalized with extensive lipid content and cholesterol crystals (Figure 2). The average size and composition of atherosclerotic plaques after 8 or 12 weeks of high-fat diet are summarized in Table 1. Fibrous cap thickness and macrophage content of plaques at 12 weeks of dietary treatment were, respectively, smaller and higher compared to those measured in mice fed the high-fat diet for 8 weeks. These changes suggest a development toward an unstable phenotype at longer time points. However, no significant differences in plaque size, fibrous cap thickness, cellular composition, and lipid and ECM deposition were found between 8 and 12 weeks of high-fat feeding.

MRI Analysis and Correlation with Histologic Results

SE and PMC, evaluated at the brachiocephalic arteries of C57/BL6 mice, did not change over time after contrast agent administration, in accordance with the lack of atherosclerotic plaques observed by histology (data not shown; $p > .05$). On the contrary, B22956/1 injection in apoE-KO

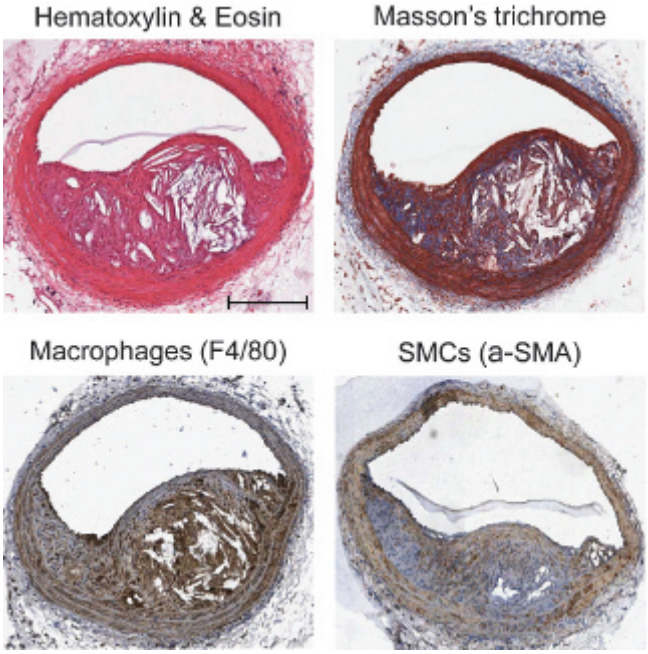

Figure 2. Histologic and immmunohistochemical characterization of atherosclerotic plaques at the brachiocephalic artery. Representative photomicrographs of hematoxylin and eosin and Masson's trichrome staining of the plaque area, as well as of immunostaining for macrophages and smooth muscle cells (SMCs), using antibodies directed against F4/80 and α-smooth muscle actin (α-SMA), respectively. Bar in top left panel = 200 μm.

Table 1. Histologic and Immunohistochemical Parameters

Parameter	*8 Weeks (mean ± SD)*	*12 Weeks (mean ± SD)*
Plaque area (μm^2)	49,680 ± 49,666	50,032 ± 27,403
Fibrous cap thickness (μm)	12.98 ± 13.73	9.79 ± 5.04
% Lumen stenosis	29.73 ± 26.31	32.55 ± 17.81
% Lipids	8.54 ± 7.82	11.43 ± 5.17
% ECM	11.19 ± 12.17	17.05 ± 10.29
% SMCs	20.37 ± 15.46	26.78 ± 13.59
% Macrophages	31.59 ± 24.46	46.02 ± 18.44

ECM = extracellular matrix; SMC = smooth muscle cell.

mice caused a rapid increase in SE and PMC mean values, which remained stable up to 70 minutes (Figure 3).

Given that histologic analysis of apoE-KO brachiocephalic arteries showed no differences between 8 and 12 weeks of high-fat feeding (see Table 1), all apoE-KO mice were considered as a single group in subsequent analyses.

Possible correlations between histologic and MRI data were assessed. Among all the histologic parameters measured, significant positive correlations were found between macrophage content or percentage of stenosis and SE or PMC, whereas a trend toward an inverse relation was observed at early time points for ECM content. Figure 4 shows correlations of SE data, obtained at different time points, with macrophage content, ECM content, and percentage of stenosis. A linear correlation between SE and macrophage content was found 10 and 40 minutes after B22956/1 injection (see Figure 4). The percentage of ECM and stenosis was not significantly correlated with SE values at each time point analyzed. Figure 5 shows two examples of apoE-KO brachiocephalic arteries visualized at MRI precontrast and 40 minutes postcontrast and analyzed by histology for macrophage content. Although both arteries showed a very high degree of stenosis, only the plaque characterized by high macrophage content was detectable after contrast agent administration (see Figure 5A). Finally, a trend toward a positive correlation between PMC and macrophage content was observed 10 minutes after contrast agent administration. Moreover, this correlation was statistically significant 40 at minutes (Figure 6). Interestingly, 70 minutes after B22956/1 infusion, PMC significantly correlated with the percentage of stenosis. No significant correlations were found between SE or PMC and lipid content, SMC content, or fibrous cap thickness (data not shown; $p > .05$).

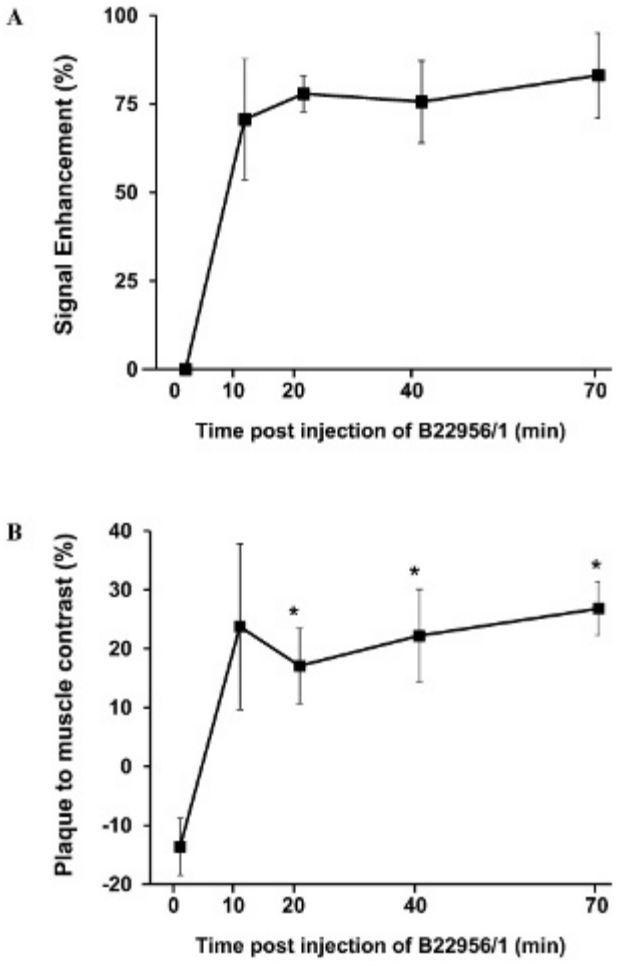

Figure 3. (A) Signal enhancement (SE) and (B) plaque to muscle contrast (PMC) measured before (0) and 10, 20, 40, and 70 minutes after intravenous injection of B22956/1 (0.1 mmol/kg). MRI data were analyzed considering all apoE-KO mice as a single group. The maximum SE was observed 10 minutes after B22956/1 injection. Starting from 20 minutes after B22956/1, a significant higher PMC was detected compared to the PMC values measured at time 0. For PMC, time 10 minutes postinjection was not included in the statistical analysis because of the low number of mice. Data are expressed as mean ± SEM. *$p < .005$ vs time 0.

Discussion

Atherosclerosis is a progressive disease of medium and large arteries that can have very diverse clinical

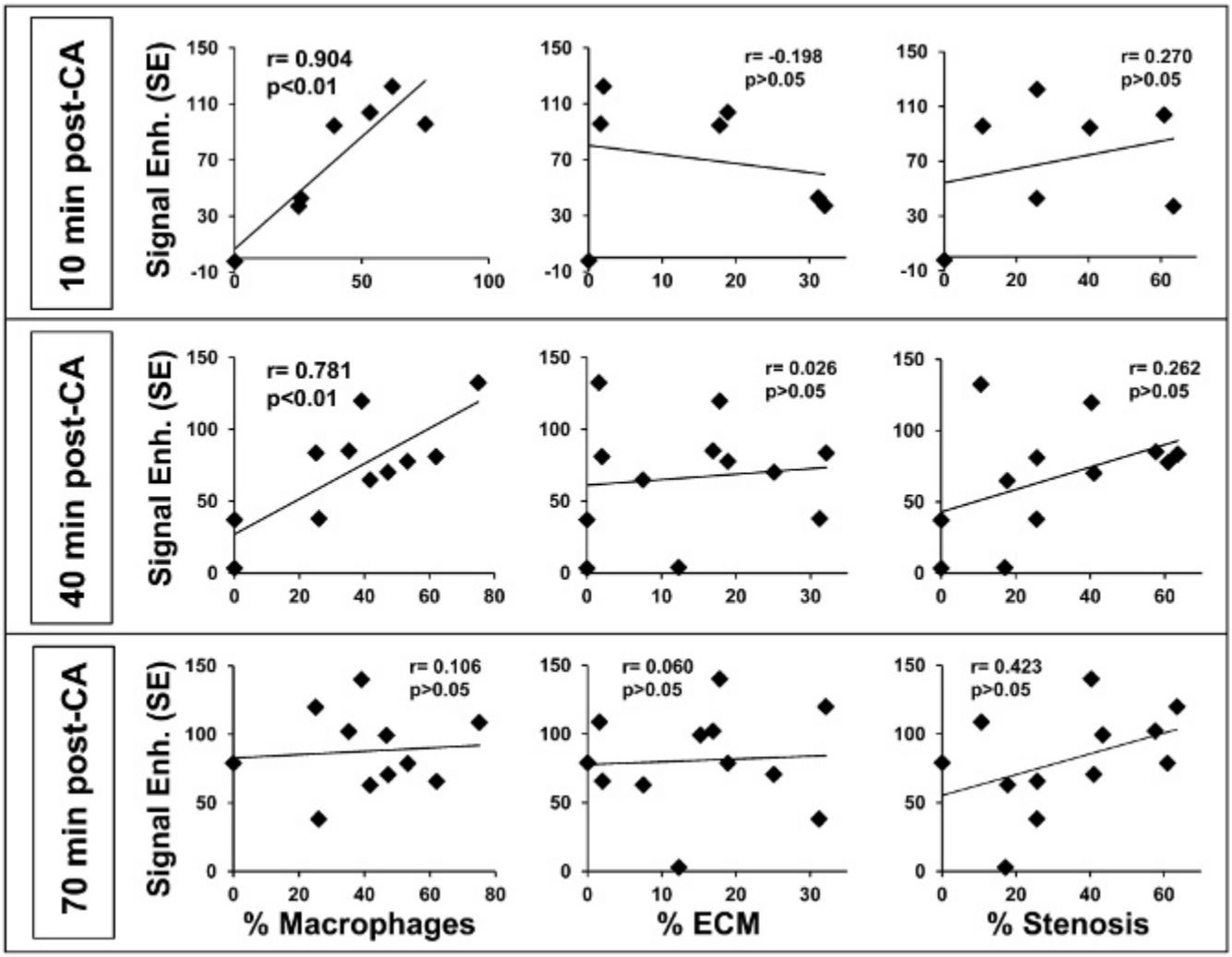

Figure 4. Correlation between signal enhancement (SE) and macrophages (%), extracellular matrix (% ECM), and stenosis (%) 10, 40, and 70 minutes post–contrast agent (CA; B22956/1) injection. The significance of correlation was calculated with the Pearson chi-square test. Ten minutes post-CA, in four animals, the quality of the MRIs did not allow reliable measurements of the plaque area; therefore, the data shown in the figure refer to seven mice.

features. Some patients experience a progressive, symptomatic disease, whereas others are totally asymptomatic and suddenly show acute clinical manifestations, such as myocardial infarction or stroke. Based on these observations, the traditional risk factors or the degree of luminal stenosis appears to be insufficient for identifying and possibly preventing acute cardiovascular events.[21] In this respect, MRI may represent a powerful tool for the noninvasive detection of high-risk patients before the onset of clinical manifestations.[22] To understand the pathologic mechanisms involved in the atherosclerotic process, several contrast agents have been developed. Gd chelates are the contrast agents most commonly used in MRI. They act by shortening the longitudinal relaxation time (T_1) and cause signal enhancement in areas of accumulation, which can be detected using T_1-weighted magnetic resonance sequences.[23] Gd-based contrast agents are used in clinical practice to evaluate tissue neovascularization in different pathologic conditions, including tumors. In the context of atherosclerosis, Gd chelates are used in magnetic resonance angiography to detect carotid stenosis.[24] However, these agents not only delineate the vessel lumen but also extravasate into the vessel wall and cause signal enhancement of arterial plaques, depending on plaque structure and composition.[25,26]

In experimental models, B22956/1 displayed a better ability to enhance atherosclerotic plaques versus other Gd-based contrast agents.[19] Thus, its potential in the visualization of vulnerable plaques was investigated.

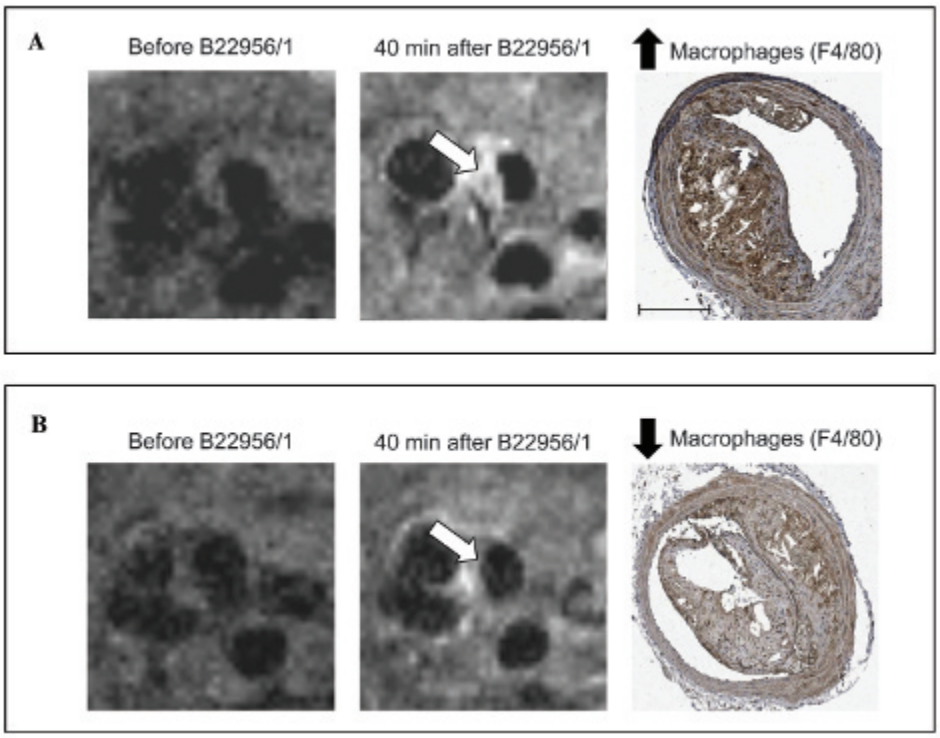

Figure 5. Corresponding sections of mouse brachiocephalic arteries from in vivo MRIs, acquired before and 40 minutes after B22956/1 injection, and ex vivo immunohistochemistry photomicrographs, using a macrophage-specific antibody (F4/80). Bar = 200 μm. A significant increase in vessel wall enhancement was observed (panel A, *white arrow*) in the plaque characterized by a high macrophage content (panel A, *black arrow*), whereas no signal enhancement was detected (panel B, *white arrow*) in the plaque characterized by a low macrophage content (panel B, *black arrow*).

For the identification of rupture-prone plaques, macrophage targeting is highly desirable because high macrophage content is a common feature of vulnerable plaques.[27] To this aim, intraplaque macrophages have been targeted by both passive and active approaches.[28,29]

The present study demonstrates the ability of B22956/1 to detect, within a short time, plaques developing at the brachiocephalic artery of apoE-KO mice, histologically resembling human vulnerable plaques. Interestingly, SE and PMC increased very rapidly, reaching the maximal value 10 minutes after the injection and remaining stable for up to 70 minutes (see Figure 2). This result differs from that described by Cornily and colleagues in rabbits, where the injection of the same dose of this contrast agent caused a progressive increase in plaque enhancement up to 90 minutes and reached a plateau between 90 and 120 minutes.[19] This timing discrepancy could be at least partially explained by a difference in the endothelial permeability of luminal endothelium and vasa vasorum between the plaques generated in the two animal models. In support of this hypothesis, it should be noted that, recently, high endothelial permeability was detected at the brachiocephalic artery of high fat–fed apoE-KO mice.[30]

B22956/1 is a blood-pool agent because it binds very rapidly and almost completely to serum albumin. This feature has been demonstrated in several animal species, including rats, where the fraction bound to albumin was calculated to be about 85%.[18] It is unlikely that the rapid and strong plaque enhancement observed in the present study is solely due to the entrance of the unbound B22956/1 fraction within the plaque. In this regard, it should be recalled that an elegant experimental study has demonstrated that fluorescently labeled albumin could pass the artery wall of atherosclerotic lesions.[31]

Endothelial permeability is generally associated with plaque inflammation.[32] Interestingly, in the present study, a strong and linear correlation was found, at early time points, between SE or PMC and plaque macrophage content, indicating the ability of this contrast agent to identify plaques with vulnerability features. It is possible that prolonged exposure to B22956/1 allowed its penetration into plaques with lower endothelial permeability and reduced inflammation, leading to a loss of correlation between SE and PMC with the macrophage content. Consistent with this observation, a loss of selectivity for vulnerable plaques at longer time points led to a significant correlation between PMC and plaque size 70 minutes postinjection (see Figure 5). Only a correlation trend was observed between SE and plaque size at the same time point.

Conclusion

B22956/1 administration to high fat–fed apoE-KO mice resulted in the enhancement of atherosclerotic plaques

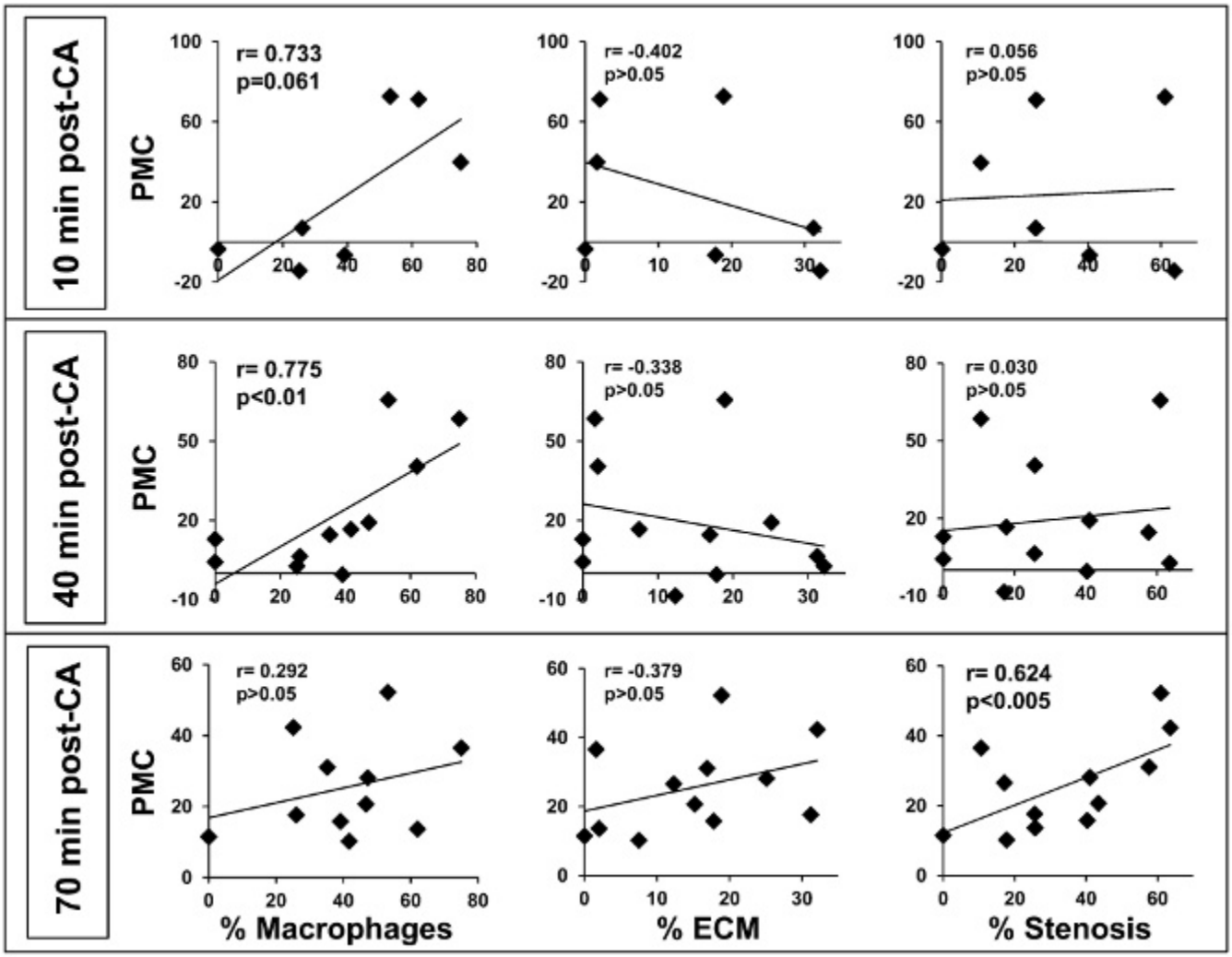

Figure 6. Correlation between plaque to muscle contrast (PMC) and macrophages (%), extracellular matrix (% ECM), and stenosis (%) 10, 40, and 70 minutes after contrast agent (CA; B22956/1) injection. The significance of correlation was calculated with the Pearson chi-square test. Ten minutes post-CA, in four animals, the quality of the MRIs did not allow reliable measurements of the plaque area; therefore, the data shown in the figure refer to seven mice.

already after 10 minutes from the injection, suggesting good suitability of this contrast agent for the evaluation of atherosclerotic plaques in patients. Moreover, B22956/1 showed a great ability to rapidly visualize vulnerable plaques, characterized by a high macrophage content. These results suggest that B22956/1, among the Gd-based contrast agents, can be considered a potentially interesting tool for the identification of atherosclerotic plaques characterized by high vulnerability and thus is prone to causing acute cardiovascular events.

Acknowledgments

We deeply thank Bracco Imaging S.p.A. (Colleretto Giacosa, Turin, Italy) for providing the contrast agent B22956/1 and Luigi Miragoli, Claudia Cabella, Giovanni Valbusa, and Fabio Tedoldi for their excellent support in MRI analyses. We also thank Marco Brevi for technical assistance in histology.

Financial disclosure of authors: This work was partially supported by a grant from the European Union (FP6 LSHM-CT2006-037498) and by the British-Italian Partnership Programme for Young Researchers (Cinzia Parolini and Jason L. Johnson).

Financial disclosure of reviewers: None reported.

References

1. Roger VL, Go AS, Lloyd-Jones DM, et al. American Heart Association Statistics Committee and Stroke Statistics Subcommittee. Heart disease and stroke statistics--2012 update: a report from the American Heart Association Circulation 2012;125:e2–220, doi:10.1161/CIR.0b013e31823ac046.

2. Virmani R, Burke AP, Farb A, Kolodgie FD. Pathology of the vulnerable plaque. J Am Coll Cardiol 2006;47:C13–8, doi:10.1016/j.jacc.2005.10.065.
3. Kolodgie FD, Virmani R, Burke AP, et al. Pathologic assessment of the vulnerable human coronary plaque. Heart 2004;90:1385–91, doi:10.1136/hrt.2004.041798.
4. Narula J, Garg P, Achenbach S, et al. Arithmetic of vulnerable plaques for noninvasive imaging. Nat Clin Pract Cardiovasc Med 2008;5 Suppl 2:S2–10, doi:10.1038/ncpcardio1247.
5. Libby P, Aikawa M. Stabilization of atherosclerotic plaques: new mechanisms and clinical targets. Nat Med 2002;8:1257–62, doi:10.1038/nm1102-1257.
6. Zadelaar S, Kleemann R, Verschuren L, et al. Mouse models for atherosclerosis and pharmaceutical modifiers. Arterioscler Thromb Vasc Biol 2007;27:1706–21, doi:10.1161/ATVBAHA.107.142570.
7. Nakashima Y, Plump AS, Raines EW, et al. ApoE-deficient mice develop lesions of all phases of atherosclerosis throughout the arterial tree. Arterioscler Thromb 1994;14:133–40, doi:10.1161/01.ATV.14.1.133.
8. Smith JD, Breslow JL. The emergence of mouse models of atherosclerosis and their relevance to clinical research. J Intern Med 1997;242:99–109, doi:10.1046/j.1365-2796.1997.00197.x.
9. Rosenfeld ME, Polinsky P, Virmani R, et al. Advanced atherosclerotic lesions in the innominate artery of the ApoE knockout mouse. Arterioscler Thromb Vasc Biol 2000;20:2587–92, doi:10.1161/01.ATV.20.12.2587.
10. Jackson CL, Bennett MR, Biessen EA, et al. Assessment of unstable atherosclerosis in mice. Arterioscler Thromb Vasc Biol 2007;27:714–20, doi:10.1161/01.ATV.0000261873.86623.e1.
11. Bond AR, Jackson CL. The fat-fed apolipoprotein E knockout mouse brachiocephalic artery in the study of atherosclerotic plaque rupture. J Biomed Biotechnol 2011;2011:379069.
12. Choudhury RP, Fuster V, Badimon JJ, et al. MRI and characterization of atherosclerotic plaque: emerging applications and molecular imaging. Arterioscler Thromb Vasc Biol 2002;22:1065–74, doi:10.1161/01.ATV.0000019735.54479.2F.
13. Corti R, Fuster V. Imaging of atherosclerosis: magnetic resonance imaging. Eur Heart J 2011;32:1709–19, doi:10.1093/eurheartj/ehr068.
14. Cai J, Hatsukami TS, Ferguson MS, et al. In vivo quantitative measurement of intact fibrous cap and lipid-rich necrotic core size in atherosclerotic carotid plaque: comparison of high-resolution, contrast-enhanced magnetic resonance imaging and histology. Circulation 2005;112:3437–44, doi:10.1161/CIRCULATIONAHA.104.528174.
15. Yuan C, Kerwin WS, Ferguson MS, et al. Contrast-enhanced high resolution MRI for atherosclerotic carotid artery tissue characterization. J Magn Reson Imaging 2002;15:62–7, doi:10.1002/jmri.10030.
16. Kerwin WS, O'Brien KD, Ferguson MS, et al. Inflammation in carotid atherosclerotic plaque: a dynamic contrast-enhanced MR imaging study. Radiology 2006;241:459–68, doi:10.1148/radiol.2412051336.
17. Kerwin WS, Hatsukami T, Yuan C, et al. MRI of carotid atherosclerosis. AJR Am J Roentgenol 2013;200:W304–13, doi:10.2214/AJR.12.8665.
18. de Haën C, Anelli PL, Lorusso V, et al. Gadocoletic acid trisodium salt (B22956/1): a new blood pool magnetic resonance contrast agent with application in coronary angiography. Invest Radiol 2006;41:279–91, doi:10.1097/01.rli.0000195848.17065.13.
19. Cornily JC, Hyafil F, Calcagno C, et al. Evaluation of neovessels in atherosclerotic plaques of rabbits using an albumin-binding intravascular contrast agent and MRI. J Magn Reson Imaging 2008;27:1406–11, doi:10.1002/jmri.21369.
20. Johnson J, Carson K, Williams H, et al. Plaque rupture after short periods of fat feeding in the apolipoprotein E-knockout mouse: model characterization and effects of pravastatin treatment. Circulation 2005;111:1422–30, doi:10.1161/01.CIR.0000158435.98035.8D.
21. Libby P. Mechanisms of acute coronary syndromes and their implications for therapy. N Engl J Med 2013;368:2004–13, doi:10.1056/NEJMra1216063.
22. Sanz J, Fayad ZA. Imaging of atherosclerotic cardiovascular disease. Nature 2008;451:953–7, doi:10.1038/nature06803.
23. Briley-Saebo KC, Mulder WJ, Mani V, et al. Magnetic resonance imaging of vulnerable atherosclerotic plaques: current imaging strategies and molecular imaging probes. J Magn Reson Imaging 2007;26:460–79, doi:10.1002/jmri.20989.
24. Anzidei M, Napoli A, Zaccagna F, et al. Diagnostic accuracy of colour Doppler ultrasonography, CT angiography and blood-pool-enhanced MR angiography in assessing carotid stenosis: a comparative study with DSA in 170 patients Radiol Med 2012;117:54–71, doi:10.1007/s11547-011-0651-3.
25. Lobatto ME, Fuster V, Fayad ZA, Mulder WJ. Perspectives and opportunities for nanomedicine in the management of atherosclerosis. Nat Rev Drug Discov 2011;10:835–52, doi:10.1038/nrd3578.
26. Calcagno C, Ramachandran S, Millon A, et al. Gadolinium-Based Contrast Agents For Vessel Wall Magnetic Resonance Imaging (MRI) of atherosclerosis. Curr Cardiovasc Imaging Rep 2013;6:11–24, doi:10.1007/s12410-012-9177-x.
27. Kanwar RK, Chaudhary R, Tsuzuki T, Kanwar JR. Emerging engineered magnetic nanoparticulate probes for targeted MRI of atherosclerotic plaque macrophages. Nanomedicine 2012;7:735–49, doi:10.2217/nnm.12.46.
28. Majmudar MD, Yoo J, Keliher EJ, et al. Polymeric nanoparticle PET/MR imaging allows macrophage detection in atherosclerotic plaques. Circ Res 2013;122:755–61, doi:10.1161/CIRCRESAHA.111.300576.
29. Lipinski MJ, Amirbekian V, Frias JC, et al. MRI to detect atherosclerosis with gadolinium-containing immunomicelles targeting the macrophage scavenger receptor. Magn Reson Med 2006;56:601–10, doi:10.1002/mrm.20995.
30. Phinikaridou A, Andia ME, Protti A, et al. Noninvasive magnetic resonance imaging evaluation of endothelial permeability in murine atherosclerosis using an albumin-binding contrast agent. Circulation 2012;126:707–19, doi:10.1161/CIRCULATIONAHA.112.092098.
31. Murphy CL, Lever MJ. Sulphorhodamine-B-labelled albumin uptake around the ostium of the renal artery in rabbits: changes with age. J Vasc Res 2002;39:104–13, doi:10.1159/000057759.
32. Badimon L, Storey RF, Vilahur G. Update on lipids, inflammation and atherothrombosis. Thromb Haemost 2011;105 Suppl 1:S34–42, doi:10.1160/THS10-11-0717.